Int. J. Heat Mass Transfer. Vol. 19, pp. 165–174. Pergamon Press 1976. Printed in Great Britain

TRANSIENT FREE CONVECTION WITH MASS TRANSFER ON AN ISOTHERMAL VERTICAL FLAT PLATE

G. D. CALLAHAN* and W. J. MARNER†
Department of Mechanical Engineering, South Dakota School of Mines and Technology, Rapid City, SD 57701, U.S.A.

(Received 16 March 1973 and in revised form 13 May 1975)

Abstract—Transient, laminar free convection along a vertical, isothermal flat plate arising from buoyancy forces created by both temperature and concentration gradients is investigated. All fluid properties, except for the temperature and concentration dependent body forces, are assumed to be constants in the analysis. Non-dimensionalization of the governing boundary layer equations results in the following parameters: (1) N, the buoyancy ratio parameter, (2) Pr, the Prandtl number, and (3) Sc, the Schmidt number. The coupled nonlinear partial differential equations are solved numerically using an explicit finite difference procedure. Results are obtained for $Pr = 1$ and a realistic range of Sc and positive N. Representative transient and steady state velocity, temperature, and concentration profiles are presented, along with transient mean Nusselt and Sherwood numbers. For short times, heat transfer is by conduction only and mass transfer is by diffusion only. Following this initial period, the body forces generate motion in the fluid and both convective heat and mass transfer become important. The transient velocity, temperature, and concentration profiles all reach maximum values before decreasing slightly to their respective steady state values. Owing to this overshoot phenomenon in the temperature and concentration profiles, a temporal minimum is observed in both the Nusselt and Sherwood numbers. For mass transfer aiding the flow, the results show that the Nusselt and Sherwood numbers are higher than those for pure thermal convection.

NOMENCLATURE

c, concentration;
C, dimensionless concentration, $(c-c_\infty)/(c_w-c_\infty)$;
c_p, constant pressure specific heat;
D, diffusion coefficient;
g, acceleration due to gravity;
Gr_L, thermal Grashof number, $\beta g L^3(T_w-T_\infty)/\nu^2$;
Gr_L^*, mass Grashof number, $\beta^* g L^3(c_w-c_\infty)/\nu^2$;
h, local heat-transfer coefficient, $-k(\partial T/\partial y)_w/(T_w-T_\infty)$;
h_D, local mass-transfer coefficient, $-D(\partial c/\partial y)_w/(c_w-c_\infty)$;
$\bar{h}$, average heat-transfer coefficient, $\frac{1}{L}\int_0^L h\,dx$;
$\bar{h}_D$, average mass-transfer coefficient, $\frac{1}{L}\int_0^L h_D\,dx$;
k, thermal conductivity;
L, length of the flat plate;
N, buoyancy ratio parameter, $\beta^*(c_w-c_\infty)/\beta(T_w-T_\infty)$;
Nu_x, local Nusselt number, hx/k;
$\overline{Nu}_L$, average Nusselt number, $\bar{h}L/k$;
Pr, Prandtl number, ν/α;
Sc, Schmidt number, ν/D;
Sh_x, local Sherwood number, $h_D x/D$;
$\overline{Sh}_L$, average Sherwood number, $\bar{h}_D L/D$;
t, time;
T, temperature;
u, x-velocity component;
U, dimensionless x-velocity component, $\frac{uL}{\nu}Gr_L^{-\frac{1}{2}}$;
v, y-velocity component;
V, dimensionless y-velocity component, $\frac{vL}{\nu}Gr_L^{-\frac{1}{4}}$;
x, spatial coordinate along the plate;
X, dimensionless spatial coordinate along the plate, x/L;
y, spatial coordinate normal to the plate;
Y, dimensionless spatial coordinate normal to the plate, $\frac{y}{L}Gr_L^{\frac{1}{4}}$.

Greek symbols

α, thermal diffusivity, $k/\rho c_p$;
β, volumetric coefficient of thermal expansion;
β^*, volumetric coefficient of expansion with concentration;
δ, momentum boundary-layer thickness;
δ_D, concentration boundary-layer thickness;
δ_t, thermal boundary-layer thickness;
$\Delta\tau$, dimensionless time-step;
ΔX, dimensionless finite difference grid spacing in the X-direction;
ΔY, dmensionless finite difference grid spacing in the Y-direction;
θ, dimensionless temperature, $(T-T_\infty)/(T_w-T_\infty)$;

*Present Address: RE/SPEC Inc., P.O. Box 725, Rapid City, SD 57701, U.S.A.
†Present Address: Heat Transfer Research, Inc., 1000 South Fremont Avenue, Alhambra, CA 91802, U.S.A.

μ, viscosity;
ν, kinematic viscosity, μ/ρ;
τ, dimensionless time, $\frac{t\nu}{L^2} Gr_L^{\frac{1}{2}}$;
ρ, density.

Subscripts
w, at the surface of the plate;
x, based on the distance from the leading edge of the plate;
∞, free stream conditions.

INTRODUCTION

EVER since the pioneering effort by Lorenz [1] in 1881, the analysis of free or natural convection has been of considerable interest to engineers and scientists. Most studies in this field have been concerned solely with thermal convection; however, as Gebhart and Pera [2] have pointed out, buoyancy effects resulting from concentration gradients in multicomponent mixtures can be just as important in generating fluid motion as can temperature gradients.

Representative fields of interest in which combined heat and mass transfer—under conditions of free convection—are important include: design of chemical processing equipment, formation and dispersion of fog, distributions of temperature and moisture over agricultural fields and groves of fruit trees, damage of crops due to freezing, and pollution of the environment.

The problem of thermal convection, a situation in which the buoyancy forces are generated only by temperature gradients, in external flows has been the subject of a large number of investigations [3–5]. It is only quite recently, however, that the problem of free convection which takes into account the buoyancy effects due to mass diffusion has been studied. Of particular interest here are those investigations dealing with external vertical flows.

Gebhart and Pera [2] obtained similarity solutions for steady, laminar flows adjacent to vertical surfaces and in plumes. Solutions were obtained for air and water for various values of the Schmidt number and for multiple buoyancy effects which both aided and opposed the flow. They have included an excellent literature review in their paper which covers virtually all of the work done in this area. More recently, Bottemanne [6] has considered steady state simultaneous heat and mass transfer along a vertical flat plate. Solutions to the boundary-layer equations were obtained only for $Pr = 0{\cdot}71$ and $Sc = 0{\cdot}63$.

The present investigation, involving the simultaneous effects of heat and mass transfer, is concerned with a numerical study of transient laminar free convection along an isothermal vertical plate which is subjected to a step-change in temperature and concentration. Of particular interest in this study is the effect of the buoyancy forces due to mass transfer on the transient velocity profiles, temperature profiles, Nusselt numbers, and Sherwood numbers.

ANALYSIS

Consider transient, laminar flow with simultaneous heat and mass transfer along an isothermal vertical flat plate. The following assumptions are made:

1. The fluid properties are assumed to be constants except for the body force terms in the momentum equation which are approximated by the Boussinesq relations.
2. The concentration c of the diffusing species in the binary mixture is very small in comparison to the other chemical species which is present.
3. Viscous dissipation in the energy equation is negligible.
4. No chemical reactions are taking place in the flow.
5. The temperature of the plate is subjected to a step change from T_∞ to T_w at time $t = 0$. Simultaneously the surface concentration is changed from a value of c_∞ to c_w.
6. The boundary-layer equations for mass, momentum, energy, and species are applicable.

Based on these assumptions the continuity, momentum, energy and species equations become

$$\frac{\partial u}{\partial x} + \frac{\partial v}{\partial y} = 0 \tag{1}$$

$$\frac{\partial u}{\partial t} + u\frac{\partial u}{\partial x} + v\frac{\partial u}{\partial y} = \nu\frac{\partial^2 u}{\partial y^2} + \beta g(T - T_\infty) + \beta^* g(c - c_\infty) \tag{2}$$

$$\frac{\partial T}{\partial t} + u\frac{\partial T}{\partial x} + v\frac{\partial T}{\partial y} = \alpha\frac{\partial^2 T}{\partial y^2} \tag{3}$$

$$\frac{\partial c}{\partial t} + u\frac{\partial c}{\partial x} + v\frac{\partial c}{\partial y} = D\frac{\partial^2 c}{\partial y^2} \tag{4}$$

where the x-coordinate is directed upward along the plate and the y-coordinate outward from the plate. The corresponding initial and boundary conditions are:

$$\begin{aligned} u(x, y, 0) &= 0 \\ u(x, 0, t) &= 0 \\ u(0, y, t) &= 0 \\ u(x, \infty, t) &= 0 \\ v(x, y, 0) &= 0 \\ v(x, 0, t) &= 0 \\ T(x, y, 0) &= T_\infty \\ T(x, 0, t) &= T_w \\ T(0, y, t) &= T_\infty \\ T(x, \infty, t) &= T_\infty \\ c(x, y, 0) &= c_\infty \\ c(x, 0, t) &= c_w \\ c(0, y, t) &= c_\infty \\ c(x, \infty, t) &= c_\infty. \end{aligned} \tag{5}$$

Equations (1)–(5) may be expressed in dimensionless form as

$$\frac{\partial U}{\partial X} + \frac{\partial V}{\partial Y} = 0 \tag{6}$$

$$\frac{\partial U}{\partial \tau} + U\frac{\partial U}{\partial X} + V\frac{\partial U}{\partial Y} = \frac{\partial^2 U}{\partial Y^2} + \theta + NC \tag{7}$$

$$\frac{\partial \theta}{\partial \tau} + U\frac{\partial \theta}{\partial X} + V\frac{\partial \theta}{\partial Y} = \frac{1}{Pr}\frac{\partial^2 \theta}{\partial Y^2} \tag{8}$$

$$\frac{\partial C}{\partial \tau}+U\frac{\partial C}{\partial X}+V\frac{\partial C}{\partial Y}=\frac{1}{Sc}\frac{\partial^2 C}{\partial Y^2} \tag{9}$$

$$\begin{aligned} U(X,Y,0)&=0\\ U(X,0,\tau)&=0\\ U(0,Y,\tau)&=0\\ U(X,\infty,\tau)&=0\\ V(X,Y,0)&=0\\ V(X,0,\tau)&=0\\ \theta(X,Y,0)&=0\\ \theta(X,0,\tau)&=1\\ \theta(0,Y,\tau)&=0\\ \theta(X,\infty,\tau)&=0\\ C(X,Y,0)&=0\\ C(X,0,\tau)&=1\\ C(0,Y,\tau)&=0\\ C(X,\infty,\tau)&=0. \end{aligned} \tag{10}$$

The dimensionless quantities are defined in the Nomenclature.

Equations (6)–(10) show that the dependent variables U, V, θ and C are functions of the dimensionless spatial coordinates X and Y, dimensionless time τ, and the dimensionless parameters N, Pr and Sc. In view of the definition of the two Grashof numbers, the parameter N may be defined as

$$N=\frac{\beta^*(c_w-c_\infty)}{\beta(T_w-T_\infty)}. \tag{11}$$

It is noted that N is equal to zero when there is no mass diffusion body force and becomes infinite when there is no thermal diffusion. Equation (7) indicates that when $N<0$, the mass diffusion buoyancy forces oppose those of thermal diffusion, when $N=0$ the buoyancy effects are purely thermal, and when $N>0$ the mass diffusion buoyancy forces aid those of thermal diffusion.

In the case of pure forced convection the Prandtl number, defined as ν/α, relates the relative thicknesses of the momentum and thermal boundary layers, δ and δ_t. Similarly, for pure forced convective mass transfer the Schmidt number, defined as ν/D, relates the momentum and concentration boundary-layer thicknesses, δ and δ_D. However, in the case of free convection in the presence of a mass diffusion contribution to the buoyancy force, the relationship among δ, δ_t and δ_D becomes extremely complex and depends on the ratio Pr/Sc as well as the buoyancy ratio parameter N.

It is customary to express heat- and mass-transfer characteristics in terms of the flux rate divided by the temperature or concentration difference causing the transfer. This ratio defines the heat- and mass-transfer coefficients h and h_D, respectively. For a uniform temperature or concentration difference over the plate, the flux is generally a variable. Therefore, local values, h and h_D, as well as average values, $\bar{h}$ and $\bar{h}_D$, are generally of interest. These values are then expressed in dimensionless form to obtain the local and average Nusselt and Sherwood numbers, respectively. In this analysis these groups, in terms of dimensionless variables, are:

$$Nu_x=-\left(\frac{\partial\theta}{\partial Y}\right)_w XGr_L^{\frac{1}{4}} \tag{12}$$

$$Sh_x=-\left(\frac{\partial C}{\partial Y}\right)_w XGr_L^{\frac{1}{4}} \tag{13}$$

$$\overline{Nu}_L=-Gr_L^{\frac{1}{4}}\int_0^1\left(\frac{\partial\theta}{\partial Y}\right)_w \mathrm{d}X \tag{14}$$

$$\overline{Sh}_L=-Gr_L^{\frac{1}{4}}\int_0^1\left(\frac{\partial C}{\partial Y}\right)_w \mathrm{d}X. \tag{15}$$

Of primary interest in this study are the effects of the mass-transfer contribution to the buoyancy force. Thus, except for a comparison with some previously published results for $Pr=7{\cdot}0$, the Prandtl number was set equal to a fixed value of one throughout this investigation. Results were obtained for Schmidt numbers of 0·2, 0·7, 1·0 and 7·0 and for values of the parameter N of 0·0, 1·0 and 2·0.

Solutions for short times

During the initial period following the step changes in the wall temperature and wall concentration, the body forces have not had sufficient time to generate any appreciable motion in the fluid. Hence, the velocity components U and V are both negligible for small τ. During this initial transient regime, the heat- and mass-transfer processes are dominated by pure heat conduction and pure mass diffusion, respectively, and equations (8) and (9) reduce to

$$\frac{\partial\theta}{\partial\tau}=\frac{1}{Pr}\frac{\partial^2\theta}{\partial Y^2} \tag{16}$$

$$\frac{\partial C}{\partial\tau}=\frac{1}{Sc}\frac{\partial^2 C}{\partial Y^2}. \tag{17}$$

Thus, for short times it is noted that for a given Prandtl number, the temperature profile is a function only of time and the normal distance from the wall. Similarly, the concentration profile is a function only of time and the normal distance from the plate for a fixed Schmidt number. Setting $Pr=1$, the solutions of equations (16) and (17), subject to the initial and boundary conditions given in equation (10), are [7]

$$\theta=\operatorname{erfc}\left[\frac{Y}{2}\left(\frac{1}{\tau}\right)^{\frac{1}{2}}\right] \tag{18}$$

$$C=\operatorname{erfc}\left[\frac{Y}{2}\left(\frac{Sc}{\tau}\right)^{\frac{1}{2}}\right] \tag{19}$$

where erfc is the complimentary error function. Using the definitions of the Nusselt and Sherwood numbers, a straightforward manipulation of equations (18) and (19) leads to the following analytical expressions for the initial transient period

$$\overline{Nu}_L/Gr_L^{\frac{1}{4}}=(1/\pi\tau)^{\frac{1}{2}} \tag{20}$$

$$\overline{Sh}_L/Gr_L^{\frac{1}{4}}=(Sc/\pi\tau)^{\frac{1}{2}}. \tag{21}$$

FINITE DIFFERENCE SOLUTION

Solutions to the coupled continuity, momentum, energy and species equations—equations (6)–(9)—subject to the initial and boundary conditions—equation (10)—were obtained using a numerical procedure. Starting from the specified initial conditions at time

$\tau = 0$, the velocity, temperature and concentration fields were obtained at time $\tau + \Delta\tau$ by using explicit finite difference approximations to the governing equations and boundary conditions.

Successive application of these finite difference expressions then yielded the transient velocity, temperature and concentration profiles and eventually steady-state conditions were approached—provided that stability requirements were satisfied. Following the method prescribed by Carnahan *et al.* [8] it can be shown, for $Pr = 1$, that the stability criterion in this case must satisfy the inequality

$$\Delta\tau \leqslant \frac{1}{N}\left[\frac{U}{\Delta X}+\frac{|V|}{\Delta Y}+\frac{1}{Sc}\frac{2}{(\Delta Y)^2}\right]^{-1} \tag{22}$$

at all discrete points in the flow field. Since both U and V vary throughout the flow, it is apparent that the critical time-step—consistent with equation (22)—is actually a variable.

In order to obtain adequate convergence, it was found necessary to take very small values of ΔY near the surface and very small values of ΔX near the leading edge of the plate. Thus, in order to keep the computing time requirements within reasonable limits, variable mesh sizes were employed in both the X- and Y-directions. All results presented in the following section were obtained using the following mesh sizes:

$$\begin{aligned}
\Delta X &= 0{\cdot}02(0 \leqslant X \leqslant 0{\cdot}10)\\
\Delta X &= 0{\cdot}06(0{\cdot}10 \leqslant X \leqslant 0{\cdot}40)\\
\Delta X &= 0{\cdot}10(0{\cdot}40 \leqslant X \leqslant 1{\cdot}00)\\
\Delta Y &= 0{\cdot}10(0 \leqslant Y \leqslant 2{\cdot}00)\\
\Delta Y &= 0{\cdot}50(2{\cdot}00 \leqslant Y \leqslant 12{\cdot}0).
\end{aligned}$$

In order to obtain a numerical solution it was necessary to limit the problem to a finite, rather than an infinite, extent in the Y-direction. Thus, after some preliminary investigations, a maximum value of $Y = 12{\cdot}0$ was chosen for computational purposes. In order to check convergence of the finite difference solutions, the spatial mesh sizes were doubled—accompanied by an appropriate change in $\Delta\tau$—and results for the two solutions were compared. The maximum difference in any of the dependent variables was observed to be seven per cent which was considered to be an acceptable degree of convergence.

Once the temperature and concentration profiles are known at any given time, the local and mean Nusselt and Sherwood numbers may be evaluated. The local heat and mass transfer coefficients were obtained using 5-point approximations for the derivatives $(\partial\theta/\partial Y)_w$ and $(\partial C/\partial Y)_w$. Integrals in equations (14) and (15) were evaluated using Simpson's rule in order to obtain values for $\overline{Nu}_L$ and $\overline{Sh}_L$.

Steady state conditions are approached asymptotically; however, the rates of heat and mass transfer are fairly sensitive indicators of the approaching steady state conditions. In this investigation steady state conditions were assumed to exist when the change, per time-step, in the local Nusselt number or local Sherwood number at $X = 1{\cdot}0$ was less than 0·04 per cent.

A more detailed analysis of the numerical procedure, along with a complete listing of the FORTRAN computer program, which was written for a CDC 3400 digital computer, may be found in [9].

RESULTS

Limiting checks

In order to assess the accuracy of the numerical procedure, several solutions which are limiting cases of the present study were compared with previously published values.

For $N = 0$ the only contribution to the body force is due to thermal diffusion and the results are directly comparable with those of Ostrach [10]. Good agreement was obtained with the steady-state local Nusselt number results of Ostrach for $Pr = 1$. Near the leading edge of the plate ($X \leqslant 0{\cdot}1$) the maximum difference was about 6·5 per cent, while at $X = 1{\cdot}0$ the difference was only 0·75 per cent. Furthermore, a comparison of mean Nusselt number results, which are of greater interest than the local values in this study, with those of Ostrach showed a difference of only 1·25 per cent. Finally, a comparison of the steady-state velocity and temperature profiles at $X = 1{\cdot}0$, again for $Pr = 1$, with those of Ostrach showed excellent agreement (well within 1 per cent) near the plate, but with an increasing error as the free stream conditions—$U = 0$ and $\theta = 0$—were approached.

Two transient free convection solutions, obtained in the absence of mass-transfer effects, were compared with corresponding values in the literature. First, transient local Nusselt numbers for $N = 0$, $X = 1{\cdot}0$ and $Pr = 1$ were compared with results from the approximate correlation of Churchill and Usagi [11]. Although the steady-state local Nusselt number at $X = 1{\cdot}0$ predicted by these investigators is 0·395, which is 1·5 per cent lower than the Ostrach value of 0·401, reasonably good agreement was obtained over the time interval of interest, $0 \leqslant \tau \leqslant 4$. Second, transient mean Nusselt numbers for $N = 0$ and $Pr = 1$ were compared with the results of Kleppe and Marner [12], and excellent agreement was noted over the entire time range, $0 \leqslant \tau \leqslant 4$.

As a final comparison, steady state local Nusselt and Sherwood numbers—including the combined buoyancy effects of thermal and mass diffusion—were compared with the results of Gebhart and Pera [2] for $N = 2{\cdot}0$ and $Pr = Sc = 7{\cdot}0$. The largest deviation was observed at $X = 0{\cdot}10$ with a difference of 4·2 per cent while excellent agreement was found at the trailing edge of the plate with a difference of only 0·75.

Based on these comparisons, it is felt that the present numerical procedure can predict both transient and steady-state results quite accurately throughout most of the flow field. The two exceptions are: (1) near the leading edge of the plate, where very large changes are taking place, and (2) near the outer edge of the boundary layers, where the boundary conditions—$U = 0, \theta = 0$ and $C = 0$—are being approached asymptotically.

Velocity, temperature and concentration profiles

Figure 1 shows the typical development of the transient dimensionless X-component of the velocity U for $Pr = 1$, $Sc = 0{\cdot}7$ and $N = 2{\cdot}0$. The profiles presented are those at the upper edge of the plate, i.e. at $X = 1{\cdot}0$. The velocity increases steadily with time, until at $\tau \doteqdot 1{\cdot}8$ when a maximum value is reached, and then decreases slightly to a steady-state value at $\tau \doteqdot 4{\cdot}0$. The somewhat surprising phenomenon of a temporal maximum in the velocity profile has been observed and discussed by several investigators for the problem of transient free convection on a vertical flat plate in the absence of mass-transfer effects. Siegel [13], based on an approximate integral analysis, was apparently the first to predict such a behavior. Later analyses by Gebhart [14], Hellums and Churchill [15] and Kleppe and Marner [12] all confirmed the findings of Siegel. In contrast to these earlier studies, however, the present problem is considerably more complex in that N and Sc, in addition to Pr, are now additional parameters. The maximum velocity apparently occurs when the buoyancy forces in the fluid are largest, and it is clear that both the magnitude of the maximum velocity and the time at which it occurs are functions of these three parameters.

The effect of the parameter N on the steady state velocity profile, again at $X = 1{\cdot}0$, is shown in Fig. 2 for $Pr = 1$ and $Sc = 1{\cdot}0$. Clearly, the contribution of mass diffusion to the buoyancy force increases the maximum velocity significantly. A comparison of Figs. 1 and 2 shows, for fixed values of Pr and N, that a decrease in the Schmidt number also increases the maximum velocity. This increase in U may be attributed to the fact that the rate of mass transfer in the fluid, which in turn influences the buoyancy force, increases as the Schmidt number decreases.

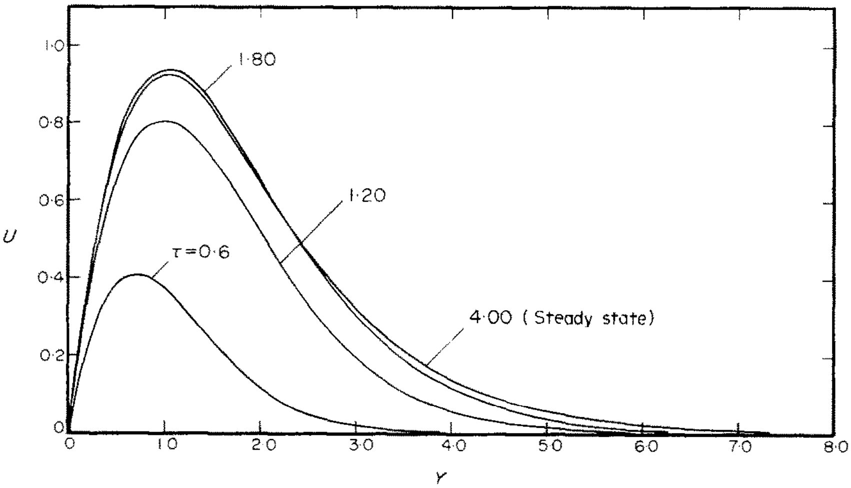

FIG. 1. Transient velocity profiles at $X = 1{\cdot}0$ for $Pr = 1{\cdot}0$, $Sc = 0{\cdot}7$, and $N = 2{\cdot}0$.

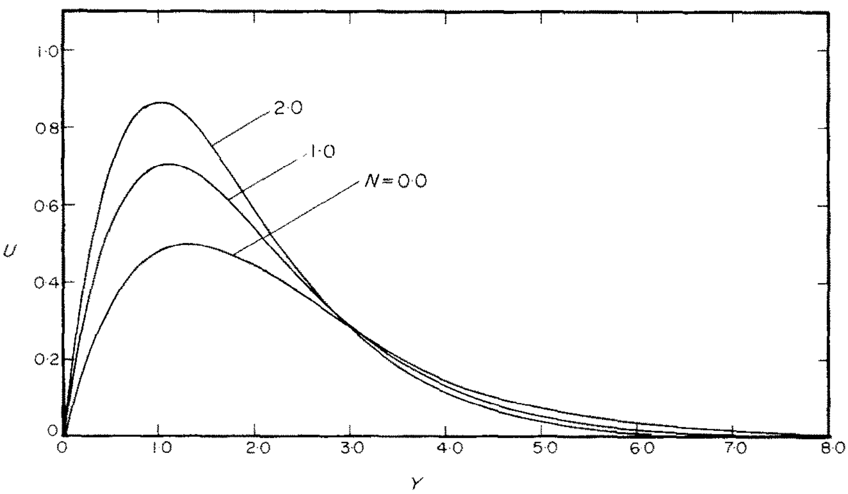

FIG. 2. Steady state velocity profiles at $X = 1{\cdot}0$ as a function of N for $Pr = Sc = 1{\cdot}0$.

Figure 3 depicts the development of the transient dimensionless temperature at $X = 1{\cdot}0$ for $Pr = 1$, $Sc = 0{\cdot}7$ and $N = 2{\cdot}0$. The temperature distribution, much as the velocity profile in Fig. 1, increases to a maximum value at $\tau \doteqdot 1{\cdot}2$ and then decreases slightly to a steady state value at $\tau \doteqdot 4{\cdot}0$. This interesting overshoot phenomenon was first predicted analytically by Siegel [13] and verified and discussed by [12, 14, 15]

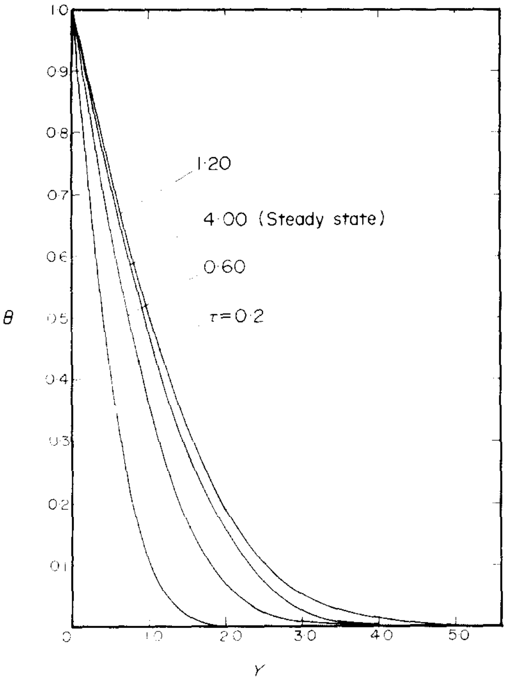

FIG. 3. Transient temperature profiles at $X = 1{\cdot}0$ for $Pr = 1{\cdot}0$, $Sc = 0{\cdot}7$ and $N = 2{\cdot}0$.

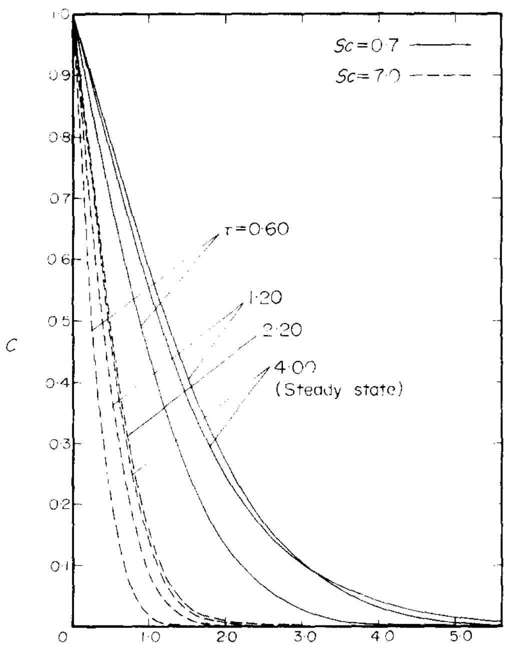

FIG. 4. Transient concentration profiles at $X = 1{\cdot}0$ for $Pr = 1{\cdot}0$, $Sc = 0{\cdot}7$ and $7{\cdot}0$, and $N = 2{\cdot}0$.

for the problem of transient free convection without mass transfer on a vertical flat plate. Experimental data obtained by Goldstein and Eckert [16] and Klei (as reported by Siegel [13]) for a vertical flat plate subjected to a step-change in heat flux also verified this phenomenon. Just as in the case of the velocity profile, the parameters N, Sc and Pr influence the extent of the overshoot in the temperature and the time at which the maximum profile occurs.

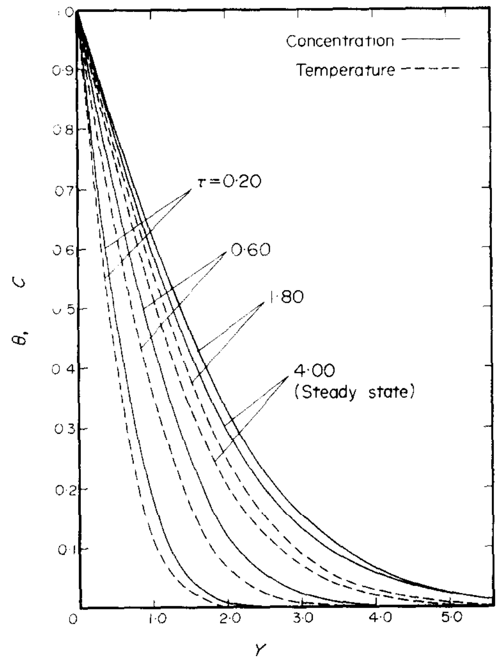

FIG. 5. Transient concentration and temperature profiles at $X = 1{\cdot}0$ for $Pr = 1{\cdot}0$, $Sc = 0{\cdot}7$ and $N = 1{\cdot}0$.

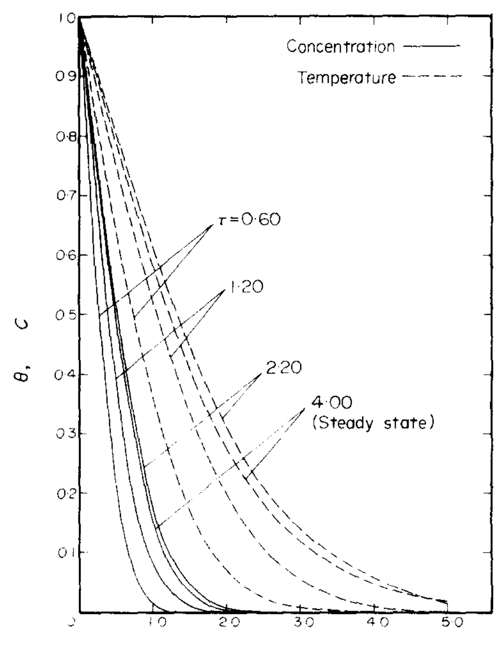

FIG. 6. Transient concentration and temperature profiles at $X = 1{\cdot}0$ for $Pr = 1{\cdot}0$, $Sc = 7{\cdot}0$ and $N = 1{\cdot}0$.

Figure 4 relates the transient concentration profiles at $X = 1{\cdot}0$ for $Pr = 1$, $Sc = 0{\cdot}7$ and $7{\cdot}0$, and $N = 2{\cdot}0$. Since the rate of mass transfer in the fluid increases with decreasing Schmidt number, the concentration boundary layer is considerably thinner for $Sc = 7{\cdot}0$ than for $Sc = 0{\cdot}7$. For a Schmidt number of $0{\cdot}7$, C increases steadily until a maximum is reached at $\tau \doteqdot 1{\cdot}20$, and then decreases to a steady-state value at $\tau \doteqdot 4{\cdot}0$. For $Sc = 7{\cdot}0$ the concentration profile reaches a maximum at $\tau \doteqdot 2{\cdot}20$ and then is observed to decrease to a steady-state value at $\tau \doteqdot 4{\cdot}0$. Thus, the overshoot previously observed in the velocity and temperature profiles is also noted here in the concentration profile. Although the maximum concentration for $Sc = 0{\cdot}7$ occurs considerably sooner than for $Sc = 7{\cdot}0$, at $\tau \doteqdot 1{\cdot}20$ as compared to $\tau \doteqdot 2{\cdot}20$, the time at which the concentration profiles reach their respective steady-state values is about the same. It should also be noted, for these values of the parameters, that the overshoot for $Sc = 0{\cdot}7$ is slightly more pronounced than for $Sc = 7{\cdot}0$.

also clearly apparent in Figs. 5 and 6 for $N = 1{\cdot}0$. Although the extent of the overshoot in both C and θ is larger for $Sc = 0{\cdot}7$ than for $7{\cdot}0$, the difference in C is clearly noticeable, while for the temperature profiles the difference is very slight.

In comparing Figs. 5 and 6, it should be noted that a change in the Schmidt number changes the concentration profile and also alters the corresponding temperature profile. This behavior reflects the coupling of the species and energy equations to the momentum equation through the temperature and concentration dependent body forces. Thus, as the body force parameter N increases, it would be expected that a corresponding influence would be observed in the velocity, temperature and concentration profiles.

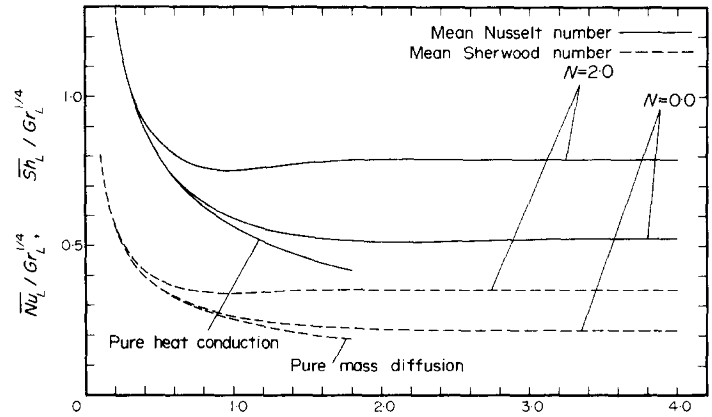

FIG. 7. The effect of N on the transient mean Nusselt and Sherwood numbers for $Pr = 1{\cdot}0$ and $Sc = 0{\cdot}2$.

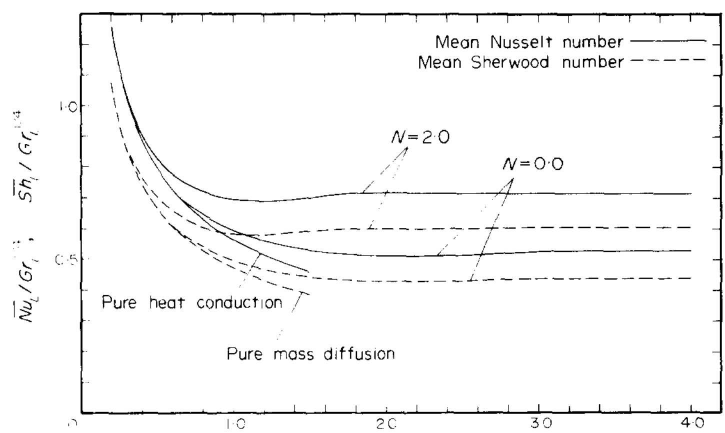

FIG. 8. The effect of N on the transient mean Nusselt and Sherwood numbers for $Pr = 1{\cdot}0$ and $Sc = 0{\cdot}7$.

A comparison of transient temperature and concentration profiles for $Pr = 1, N = 1{\cdot}0$ and $Sc = 0{\cdot}7$ and $7{\cdot}0$ is presented in Figs. 5 and 6. Note that the concentration boundary layer in Fig. 5 is thicker than the thermal boundary layer ($Pr = 1, Sc = 0{\cdot}7$), while in Fig. 6 the thermal boundary layer is considerably thicker than the concentration boundary layer ($Pr = 1$, $Sc = 7{\cdot}0$). Thus, the effect of a reduced rate of mass diffusion in the fluid as the Schmidt number increases is very apparent. It should also be noted that the overshoot in the temperature and concentration profiles previously observed in Figs. 3 and 4 for $N = 2{\cdot}0$ is

Nusselt and Sherwood numbers

Transient mean Nusselt and Sherwood numbers are shown in Figs. 7–10 for $Sc = 0{\cdot}2$, $0{\cdot}7$, $1{\cdot}0$ and $7{\cdot}0$, respectively. In each case $Pr = 1$ and $N = 0{\cdot}0$ and $2{\cdot}0$. At small times the parameter N has negligible influence on both $\overline{Nu}_L/Gr_L^{\frac{1}{4}}$ and $\overline{Sh}_L/Gr_L^{\frac{1}{4}}$ due to the fact that heat is transferred by conduction only and mass is transferred by diffusion only during this regime. Analytical expressions for the Nusselt number and the Sherwood number during this initial regime are presented in equations (20) and (21), respectively, and are shown graphically in Figs. 7–10 for comparison. As the buoyancy forces due to mass transfer and thermal convection increase, the velocity increases sufficiently for N to become a parameter. Owing to the fact that the temperature and concentration profiles reach a maximum before steady-state conditions are reached, a transient minimum is observed in both the Nusselt number and the Sherwood number. The difference

parameter N. In Fig. 9 it should be pointed out that when $Pr = Sc = 1{\cdot}0$, the temperature and concentration profiles are identical and hence the curves for the Nusselt and Sherwood numbers coincide.

As the Schmidt number increases from a value of 0·2 to a value of 7·0, a definite trend is apparent. With the Prandtl number fixed at a value of one, an increase in the Schmidt number is observed to (1) increase the Sherwood number substantially, and (2) decrease the Nusselt number moderately. Furthermore, the effect of the parameter N on the Nusselt number is noted to

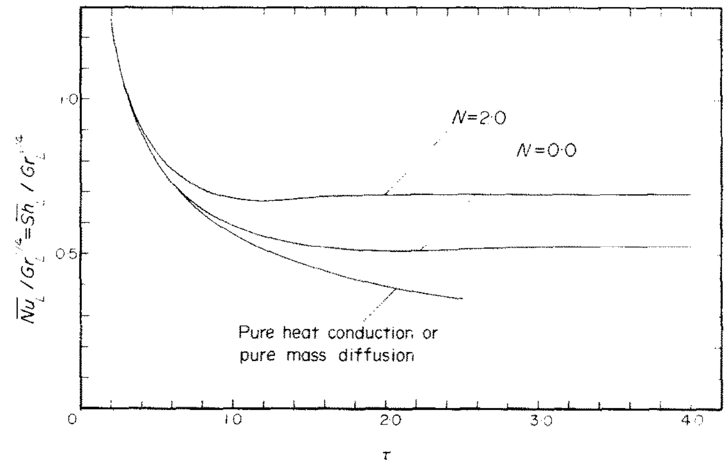

FIG. 9. The effect of N on the transient mean Nusselt and Sherwood numbers for $Pr = 1{\cdot}0$ and $Sc = 1{\cdot}0$.

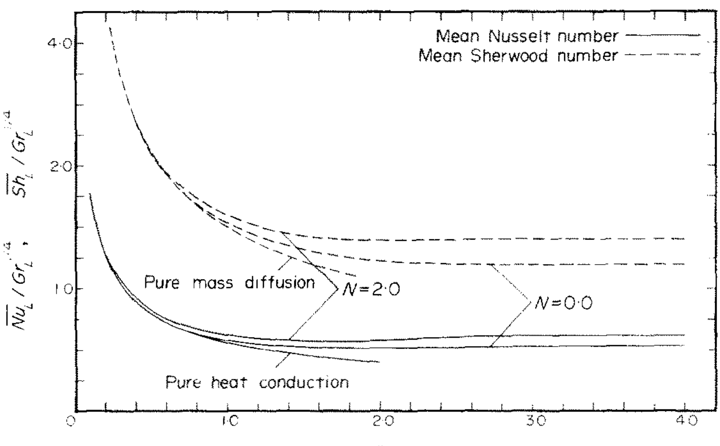

FIG. 10. The effect of N on the transient mean Nusselt and Sherwood numbers for $Pr = 1{\cdot}0$ and $Sc = 7{\cdot}0$.

between the temporal minimum and the steady-state value, however, is quite small and, in some cases, is nearly imperceptible on the figures. When N does become a parameter, it is noted that an increase in N results in higher Nusselt and Sherwood numbers. In other words, the effect of increasing the buoyancy force due to mass transfer is an increase in the rates of heat and mass transfer. In Figs. 7–10 both $\overline{Nu}_L/Gr_L^{\frac{1}{4}}$ and $\overline{Sh}_L/Gr_L^{\frac{1}{4}}$ show a slight dependence on the time required to reach steady state conditions, i.e. as Sc increases the time increases. However, the time required to reach steady-state conditions is virtually insensitive to the become less pronounced with increasing Schmidt number. As Sc increases the difference between the Nusselt number at $N = 2{\cdot}0$ and $N = 0{\cdot}0$ becomes smaller. However, just the opposite effect is observed in the case of the Sherwood number. The following explanation attempts to account for this behavior. In Fig. 4 it was observed that an increase in the Schmidt number tends to decrease the concentration boundary-layer thickness. However, even though the conservation equations are coupled, the thermal boundary-layer thickness is not highly sensitive to increases in the Schmidt number for a fixed value of the Prandtl number. Thus, as the Schmidt number increases the concentration boundary-layer thickness becomes smaller than the thermal boundary-layer thickness. Consequently, buoyancy effects due to mass transfer are diminished in the thermal boundary layer, and hence the influence of the parameter N on $\overline{Nu}_L/Gr_L^{\frac{1}{4}}$ diminishes with increasing Schmidt number. On the other hand, as the Schmidt number increases, the buoyancy effects due to thermal convection become less important in comparison to those due to mass transfer in the thinner concentration boundary layer. Hence, as the Schmidt number increases, the influence of N on $\overline{Sh}_L/Gr_L^{\frac{1}{4}}$ also increases.

CONCLUSIONS

The problem of transient laminar free convection along a vertical, isothermal flat plate arising from buoyancy forces created by both temperature and concentration gradients has been analyzed. Briefly, the most important results and conclusions may be summarized as follows:

1. For constant properties, except in the temperature and concentration dependent body force terms, the parameters of the problem are: Pr, the Prandtl number; Sc, the Schmidt number; and N, the buoyancy ratio parameter.
2. For short times the heat transfer is by conduction only, the mass transfer is by diffusion only, and both phenomena may be predicted with closed form analytical solutions.
3. Following the initial conduction–diffusion regime, motion in the fluid is generated by the two body forces. In order to obtain a solution to this problem, the governing conservation equations, which are coupled, must be solved numerically.
4. The transient velocity, temperature and concentration profiles all reach maximum values before decreasing slightly to their respective steady state values.
5. Owing to the transient overshoot in the temperature and concentration profiles, both the Nusselt and Sherwood numbers pass through a temporal minimum before reaching their steady state values.
6. For mass diffusion aiding the flow ($N > 0$), both $\overline{Nu}_L$ and $\overline{Sh}_L$ are higher than the values for pure thermal convection.

REFERENCES

1. L. Lorenz, Über das Leitungsvermogen der Metalle für Wärme und Electricität, *Wiedemanns Annelen* **13**, 582–606 (1881).
2. B. Gebhart and L. Pera, The nature of vertical natural convection flows resulting from the combined buoyancy effects of thermal and mass diffusion, *Int. J. Heat Mass Transfer* **14**, 2025–2050 (1971).
3. D. V. Julian and R. G. Akins, Bibliography of natural convection heat transfer from a vertical flat plate, *Kansas State Univ. Bull.* **51**, Special Report 77 (1967).
4. A. J. Ede, Advances in free convection, in *Advances in Heat Transfer*, Vol. 4, pp. 1–64, edited by T. F. Irvine, Jr. and J. P. Hartnett. Academic Press, New York (1967).
5. B. Gebhart, External natural convection flows, *Appl. Mech. Rev.* **22**, 691–701 (1969).
6. F. A. Bottemanne, Theoretical solution of simultaneous heat and mass transfer by free convection about a vertical flat plate, *Appl. Scient. Res.* **25**, 137–149 (1971).
7. H. S. Carslaw and J. C. Jaeger, *Conduction of Heat in Solids*, 2nd Edn. Oxford University Press, London (1959).
8. B. Carnahan, H. A. Luther and J. O. Wilkes, *Applied Numerical Methods*. John Wiley, New York (1969).
9. G. D. Callahan, Transient free convection with mass transfer on an isothermal vertical flat plate, MS thesis, South Dakota School of Mines and Technology (1972).
10. S. Ostrach, An analysis of laminar free convection flow heat transfer about a flat plate parallel to the direction of the generating body force, NACA Report 1111, 63–79 (1953).
11. S. W. Churchill and R. Usagi, A standardized procedure for the production of correlations in the form of a common empirical equation, *I/EC Fundamentals* **13**, 39–44 (1974).
12. J. Kleppe and W. J. Marner, Transient free convection in a Bingham plastic on a vertical flat plate, *J. Heat Transfer* **94C**, 371–376 (1972).
13. R. Siegel, Transient free convection from a vertical flat plate, *Trans. Am. Soc. Mech. Engrs.* **80**, 347–359 (1958).
14. B. Gebhart, Transient natural convection from vertical elements, *J. Heat Transfer* **83C**, 61–70 (1961).
15. J. D. Hellums and S. W. Churchill, Transient and steady state, free and natural convection, numerical solutions: Part 1. The isothermal, vertical plate, *A.I.Ch.E. Jl* **8**, 690–692 (1962).
16. R. J. Goldstein and E. R. G. Eckert, The steady and transient free convection boundary layer on a uniformly heated vertical plate, *Int. J. Heat Mass Transfer* **1**, 208–218 (1960–61).

CONVECTION LIBRE TRANSITOIRE AVEC TRANSFERT MASSIQUE SUR UNE PLAQUE PLANE VERTICALE ET ISOTHERME

Résumé—On étudie la convection libre laminaire transitoire résultant des forces de gravité créées par les gradients de température et de concentration sur une plaque plane verticale isotherme. Toutes les propriétés du fluide sont supposées constantes, excepté les forces de volume dépendant de la température et de la concentration. Les équations fondamentales de la couche limite rendues adimensionnelles conduisent aux paramètres suivants: (1) N, paramètre des effets de gravité, (2) Pr, nombre de Prandtl, et (3) Sc, nombre de Schmidt. Les équations aux dérivées partielles non linéaires couplées sont résolues numériquement à l'aide d'une procédure explicite de différences finies. Les résultats sont obtenus pour $Pr = 1$ et dans un domaine réaliste de Sc et N positif. On présente les profils de vitesses, températures et concentrations dans la période transitoire et à l'état permanent, ainsi que les nombres de Nusselt et de Sherwood locaux à l'état permanent. Pour des temps courts, le transfert de chaleur se fait par conduction uniquement et le transfert de masse par diffusion uniquement. Après cette période initiale, les forces de volume engendrent le mouvement du fluide et les transferts de chaleur et de masse par convection deviennent tous deux importants. Les profils de vitesses, températures et concentrations atteignent tous une valeur maximale avant de décroitre légèrement jusqu'à leurs valeurs respectives à l'état stationnaire. Ce phénomène de dépassement dans les profils de température et de concentration a pour conséquence un minimum dans le temps des nombre de Nusselt et de Sherwood. Lorsque le transfert de masse s'ajoute à l'écoulement, les résultats montrent que les nombres de Nusselt et de Sherwood sont supérieurs à ceux obtenus en convection thermique pure.

INSTATIONÄRE FREIE KONVEKTION MIT STOFFÜBERGANG AN EINER ISOTHERMEN, SENKRECHTEN, EBENEN PLATTE

Zusammenfassung—Die Untersuchung gilt der von Temperatur- und Konzentrationsgradienten erzeugten instationären, laminaren, freien Konvektion an einer senkrechten, isothermen, ebenen Platte. In der Analyse sind alle Eigenschaften des Fluids mit Ausnahme der Temperatur und der Konzentration als konstant angenommen. Aus den charakteristischen Grenzschichtgleichungen ergaben sich folgende Parameter: (1) N, das Auftriebsverhältnis, (2) Pr, die Prandtl-Zahl und (3) Sc, die Schmidt-Zahl.

Die gekoppelten, nicht-linearen, partiellen Differentialgleichungen werden numerisch gelöst mit einer Methode der finiten Elemente. Ergebnisse sind wiedergegeben für $Pr = 1$ und einen realistischen Bereich von Sc und positivem N. Zusammen mit lokalen Nusselt- und Sherwood-Zahlen für den stationären Bereich werden instationäre und stationäre Geschwindigkeiten, Temperaturen und Konzentrationsprofile angegeben. Für kurze Zeiten erfolgt der Wärmeübergang nur durch Leitung und der Massentransport nur durch Diffusion. Anschließend an diese Anlaufperiode erzeugen die Massenkräfte eine Bewegung im Fluid, und konvektiver Wärme- und Stoffübergang werden bedeutsam. Die instationären Geschwindigkeits-, Temperatur- und Konzentrationsprofile erreichen alle einen Maximalwert, ehe sie auf ihre entsprechenden stationären Werte allmählich absinken. Aufgrund dieses Überlaufphänomens der Temperatur- und der Konzentrationsprofile erreichen sowohl die Nusselt- wie auch die Sherwood-Zahl ein kurzzeitiges Minimum. Für den Fall, daß der Stoffübergang die Strömung unterstützt, liefern die Ergebnisse höhere Nusselt- und Sherwood-Zahlen als für den Fall rein thermischer Konvektion.

НЕСТАЦИОНАРНАЯ СВОБОДНАЯ КОНВЕКЦИЯ ПРИ НАЛИЧИИ МАССООБМЕНА НА ИЗОТЕРМИЧЕСКОЙ ВЕРТИКАЛЬНОЙ ПЛОСКОЙ ПЛАСТИНЕ

Аннотация — В работе рассматривается нестационарная ламинарная свободная конвекция вдоль вертикальной изотермической плоской пластины за счет подъемных сил, создаваемых градиентами температуры и концентрации.

Предполагается, что все свойства жидкости, за исключением массовых сил, зависящих от температуры и концентрации, постоянны. Приведение уравнений пограничного слоя к безразмерному виду дает следующие параметры: (1) N, параметр соотношения подъемных сил; (2) Pr, число Прандтля и (3) Sc, число Шмидта. Система нелинейных дифференциальных уравнений в частных производных решается численно с помощью явной конечно-разностной схемы. Результаты получены для $Pr = 1$, реального диапазона Sc и положительного N. Представлены характерные профили нестационарной и стационарной скорости, температуры и концентрации вместе со стационарными локальными числами Нуссельта и Шервуда. В течение начального периода времени теплообмен осуществляется только теплопроводностью, а массообмен — только диффузией. Затем массовые силы вызывают движение в жидкости, и конвективный тепло- и массообмен становится значительным. Все профили нестационарной скорости, температуры и концентрации достигают максимальных величин, а потом несколько снижаются до соответствующих стационарных значений. Вследствие этого наблюдается минимум для значений чисел Нуссельта и Шервуда.

Для случая интенсификации течения массообменом результаты показывают, что числа Нуссельта и Шервуда выше, чем при чистой тепловой конвекции.